

The calculations of Nucleon Electric Dipole Moment using background field on Lattice QCD

Fangcheng He,^{a,*} Michael Abramczyk,^b Tom Blum,^b Taku Izubuchi,^{c,d} Hiroshi Ohki^e
and Sergey Syritsyn^a

^a*Department of Physics and Astronomy, Stony Brook University,
Stony Brook, NY 11794, USA*

^b*Physics Department, University of Connecticut,
Storrs, Connecticut 06269, USA*

^c*RIKEN/BNL Research Center, Brookhaven National Laboratory,
Upton, NY 11973, USA*

^d*Physics Department, Brookhaven National Laboratory,
Upton, New York 11973, USA*

^e*Department of Physics, Nara Women's University, Nara 630-8506, Japan*

E-mail: fangcheng.he@stonybrook.edu

Measurements of nucleon and nuclei Electric Dipole Moments (EDMs) play an important role in probing CP violation and exploring physics beyond the Standard Model. We extract the neutron EDM by measuring the energy shift of the nucleon two-point correlation function in the presence of a background field. The UV divergence of the topological charge density operator is mitigated using gradient flow, and the diffusion effect induced by the gradient flow process is included into the fit ansatz. Our calculations were carried out on two 2+1 DWF fermion, Iwasaki, gauge field ensembles generated by the RBC/UKQCD collaborations with inverse lattice spacing 1.73 GeV and pion masses of about 340 and 420 MeV.

*The 40th International Symposium on Lattice Field Theory (Lattice 2023)
July 31st - August 4th, 2023
Fermi National Accelerator Laboratory*

*Speaker

1. Introduction

The nucleon electric dipole moment (nEDM) is an important indicator of CP(T)-symmetry violation. The nEDM prediction from the Standard Model's CKM matrix for the neutron is $\approx 10^{-31}$ [e cm], which is much smaller than the upper-limit determined through experiments on neutrons (ILL) [1] and ^{199}Hg [2]. The SM prediction is also too small to explain the matter-antimatter asymmetry compared to what is required by the Sakharov conditions. Hence, the measurement of the nEDM is important in the search for physics beyond Standard Model.

Strong interactions may be a source of CP violation known as the QCD " θ -term", $S_\theta = \theta Q$, where Q is the topological charge. Its contributions to the nEDM can be studied systematically from first principles only using lattice QCD. Many efforts have been made to calculate the nEDM using Lattice QCD [3–13]. In earlier calculations, an incorrect definition of the electric dipole form factor F_3 resulted in significant mixing with the Pauli form factor [9]. After subtracting the mixing term, those nEDM results became much smaller, comparable with phenomenology, and universally dominated by statistical noise even with unphysical heavy quark masses.

Currently, most of nEDM calculations on a lattice use the traditional form factor method in which nEDMs are extracted as electric dipole form factors (EDFF) $F_3(Q^2)$ from CP -odd corrections to matrix elements of the quark vector current due to topological charge. This form factor has to be extrapolated to the forward limit ($Q^2 \rightarrow 0$) to obtain the nEDM. The other method is to calculate the EDM from the nucleon energy shift $\Delta E \propto d_N(2\vec{S} \cdot \vec{E})$ in a uniform background electric field [9, 14, 15]. This method has significant advantages: no forward limit is required, there is no parity mixing between F_2 and F_3 , and one only needs to calculate the CP -odd part of the two- instead of three-point function.

We present our θ -nEDM results using the background field method. Details of this method were first described in Ref. [16]. The background field method is described in Sec. 2, the results are presented in Sec. 3, and discussed in Sec 4.

2. Electric dipole moment from background field method

In this section, we discuss and compare methods to compute the nEDM on a lattice. The form factor method has been described in multiple publications (see, e.g., Ref.[9] and references therein). The EDFF is defined as

$$\langle p', \sigma' | J^\mu | p, \sigma \rangle_{\mathcal{CP}} = \bar{u}_{p', \sigma'} \left[F_1(Q^2) \gamma^\mu + (F_2(Q^2) + iF_3(Q^2) \gamma_5) \frac{i\sigma^{\mu\nu} q_\nu}{2M_N} \right] u_{p, \sigma} \quad (1)$$

where $Q^2 = -(p' - p)^2$, and $F_{1,2,3}$ are the Dirac, Pauli, and electric dipole form factors. The forward limit of the latter yields the nEDM, $F_3(0) = 2m_n d_n$. Although the nucleon states in QCD vacuum with CP -violation are no longer parity eigenstates, it is crucial to ensure that their spinors satisfy the positive-parity Dirac equation with real-valued mass, $(\not{p} - m_N)u_{p, \sigma} = 0$, otherwise F_3 receives a spurious contribution from F_2 [9],

$$\tilde{F}_3(Q^2) = F_3 \cos(2\alpha) - F_2 \sin(2\alpha), \quad (2)$$

where α is the parity mixing of the lattice nucleon spinor due to CP -violation that can be extracted from the two-point function.

Another approach to calculate the nucleon EDM is the background field method introduced in [14–17]. It has also been extended to analyze CP-even properties, such as the electric polarizability and magnetic moments of the nucleon [18, 19]. Since the proton accelerates in an electric field, and requires a more sophisticated analysis, we study only the neutron EDM in this work. After including the background field, the Dirac equation for the parity-positive neutron spinor u_N in the rest frame ($p_N = (m_N, \vec{0})$) becomes in Euclidean space [9]

$$\left[i\not{p} + m_N - \left(\frac{1}{2} F_{\mu\nu} \sigma^{\mu\nu} \right) \frac{\kappa + i\zeta\gamma_5}{2m_N} \right] u_N = \begin{pmatrix} m_N - \frac{(\kappa+i\zeta)\vec{\mathcal{E}}\cdot\vec{\sigma}}{2m_N} & -E_N \\ -E_N & m_N + \frac{(\kappa-i\zeta)\vec{\mathcal{E}}\cdot\vec{\sigma}}{2m_N} \end{pmatrix} u_N = 0, \quad (3)$$

where E_N is the neutron energy, $\kappa, \zeta = F_{2,3}(0)$ are magnetic and electric dipole moments, and $\vec{\mathcal{E}}$ is the Euclidean electric field. To the order linear in κ, ζ , the nucleon energy E_N is

$$E_N^2 = m_N^2 - i\zeta(\vec{\Sigma} \cdot \vec{\mathcal{E}}) + O(\kappa^2, \zeta^2), \quad \text{or} \quad E_N = m_N - \frac{i\zeta}{2m_N}(\vec{\Sigma} \cdot \vec{\mathcal{E}}) + O(\kappa^2, \zeta^2) \quad (4)$$

where $\zeta/(2m_N) = d_N$ is the electric dipole moment and $\vec{\Sigma} = \text{diag}[\vec{\sigma}, \vec{\sigma}]$ is the spin operator. Note that the linear part of the energy shift $\delta E = -\frac{i\zeta}{2m_N}(\vec{\Sigma} \cdot \vec{\mathcal{E}})$ is imaginary because of the analytic continuation in electric field on a Euclidean lattice, implying that the correlation function acquires a complex phase. Expanding the path integral in $\theta \ll 1$, one obtains the CP-violating correction to the nucleon correlation function in the background field \mathcal{E} on one hand, and the t -linear correction on the other:

$$C_{2pt, \mathcal{E}, \theta} \approx \langle N(t)\bar{N}(0) \rangle_{\mathcal{E}} - i\theta \langle Q N(t)\bar{N}(0) \rangle_{\mathcal{E}} \propto e^{-Et} [1 - t\delta E + O(\theta^2)]. \quad (5)$$

The nEDM $\zeta = F_3(0)$ can be extracted from nucleon correlators in an electric field $\vec{\mathcal{E}} = \mathcal{E}_z \hat{z}$ as

$$\frac{\zeta}{\theta} = i \frac{2m_N}{\mathcal{E}_z} \frac{\delta E}{\theta} = -\frac{2m_N}{\mathcal{E}_z} \frac{d}{dt} \frac{\text{Tr}[T_{S_z}^+ \langle Q N(t)\bar{N}(0) \rangle_{\mathcal{E}_z}]}{\text{Tr}[T^+ \langle N(t)\bar{N}(0) \rangle_{\mathcal{E}_z}]}, \quad (6)$$

where $T^+ = \frac{1}{2}(1 + \gamma_4)$ is the positive-parity projector, and $T_{S_z}^+ = T^+ \cdot (1 + \Sigma_z)$ is the spin- \hat{z} projector.

So far, we have ignored excited states and negative parity state. In practice, a multi-state model can be fitted to the time dependence of the EDM estimator (6). On the other hand, the formula (6) resembles the ‘‘summation’’ method of computing ground-state matrix elements. This relation is made apparent by the Feynman-Hellman theorem (recently discussed in Ref. [20] in the context of lattice QCD), so the EDM can alternatively be calculated from the matrix element of the local density of topological charge,

$$\frac{\zeta}{\theta} = -\frac{2m_N}{\mathcal{E}_z} \langle N_{\uparrow} | q | N_{\uparrow} \rangle_{\mathcal{E}_z} \approx -\frac{2m_N}{\mathcal{E}_z} \frac{\text{Tr}[T_{S_z}^+ \langle N(t_f) q(\tau) \bar{N}(0) \rangle_{\mathcal{E}_z}]}{\text{Tr}[T^+ \langle N(t_f) \bar{N}(0) \rangle_{\mathcal{E}_z}]}. \quad (7)$$

Thus, the problem is reduced from computing a 4-point function between the nucleon fields N, \bar{N} , the global topological charge $Q = \int d^4x q(x)$, and the vector current $J_\mu = \bar{\psi} \gamma_\mu \psi$ to a correlator of N, \bar{N} and the local topological charge density $q(x)$ in uniform field:

$$C_3(t_f, \tau) = \text{Tr}[T_{S_z}^+ \langle N(t_f) q(\tau) \bar{N}(0) \rangle_{\mathcal{E}_z}] = [T_{S_z}^+]_{\beta\alpha} \sum_{\vec{y}, \vec{z}} \langle N_\alpha(t_f, \vec{y}) q(\tau, \vec{z}) \bar{N}_\beta(0) \rangle. \quad (8)$$

This point is crucial to reducing fluctuations in correlators with any operator that leads to “disconnected” Wick contractions: topological charge, Weinberg 3-gluon interaction, isoscalar 2-quark and 4-quark interactions, and so on. In this paper we concentrate on the topological charge but the methodology can be readily extended to these other \mathcal{CP} interactions.

Chiral symmetry is important for calculations involving topological charge. We use gauge configurations generated with $N_f = 2 + 1$ flavors of domain wall fermions (DWF) [21]. (Tab. 1).

Table 1: Gauge ensembles used in this work [21].

	size	m_l/m_s	m_π MeV	N_{cfg}
I24_m010	$24^3 \times 64$	0.01/0.04	432	1100
I24_m005	$24^3 \times 64$	0.005/0.04	340	1400

Periodicity on a lattice in space and time requires quantization of abelian field flux $Q_q E_k L_k L_4 = 2\pi n$, where $Q_u = \frac{2}{3}$ and $Q_d = -\frac{1}{3}$ are quark charges. A uniform electric field on the lattice is introduced by multiplying the gauge links by the $U(1)$ phase [18],

$$A_{x,4} = n_{k4} \Phi_{k4} x_k, \quad A_{x,k} |_{x_k=L_k-1} = -n_{k4} \Phi_{k4} L_k x_4, \quad (9)$$

where $n_{\mu\nu}$ is the number of quanta and $\Phi_{\mu\nu} = \frac{6\pi}{L_\mu L_\nu}$ is the unit of flux through plaquette $(\mu\nu)$. Such potentials result in a uniform electric field $\vec{E} = (n_{14} \Phi_{14}, n_{24} \Phi_{24}, n_{34} \Phi_{34})$.

3. Numerical results

To calculate nucleon correlators, we use all-mode-averaging (AMA) [22] by combining high-precision and truncated-CG samples computed with low-mode deflation of the preconditioned Dirac operator. We also employ low-mode averaging whereby we approximate the full-volume average of nucleon correlators from low modes and combine it with AMA samples to correct bias, which have resulted in a 50% reduction of statistical errors:

$$\langle \mathcal{O} \rangle \approx \langle \mathcal{O}^{\text{LMA}} \rangle_{V_4} + \langle \mathcal{O}^{\text{approx}} - \mathcal{O}^{\text{LMA}} \rangle_{N_{\text{approx}}} + \langle \mathcal{O}^{\text{exact}} - \mathcal{O}^{\text{approx}} \rangle_{N_{\text{exact}}}. \quad (10)$$

In addition, we average over spin orientations $2S_z = \pm 1$ and electric fields $\mathcal{E}_z = \pm 1, \pm 2$.

To use the Feynman-Hellman method, we need to determine the local topological charge density $q(x)$. We calculate $q(x)$ using 5-loop improved discretization [23] and gradient flow [24]. Gradient flow helps suppress $O(a)$ size dislocations that contribute to fluctuation of the global topological charge. At large enough gradient flow time, the *global topological charge* Q becomes constant. However, the *local density* (summed over the spatial volume) entering the correlator in Eq. (7), becomes delocalized (“diffused”) in the Euclidean time, which complicates analysis of its ground-state matrix elements. This effect is visible in the plateaus for d_n/θ (7) shown in Fig. 1 for source-sink separations $t = (6 \dots 10)a$: as the gradient flow time t^{gf} is increased, the τ -dependent features in the ratios (7) become more diffused. In particular, it becomes hard to isolate the ground-state plateau from the contact term contributions where the density $q(x)$ overlaps with the nucleon operators.

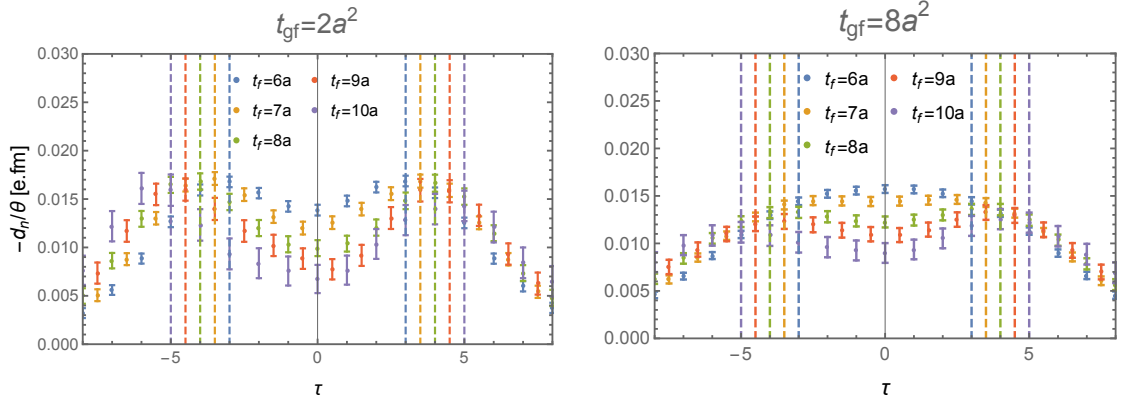


Figure 1: Plateaus of neutron matrix elements of topological charge density converted to EDM (7), depending on the gradient flow time. The vertical dashed lines of respective colors show the locations of the nucleon fields, which lead to contact terms with the gluon operator on the same time slices. As the gradient flow time increases, the contact terms “diffuse” into the EDM plateaus.

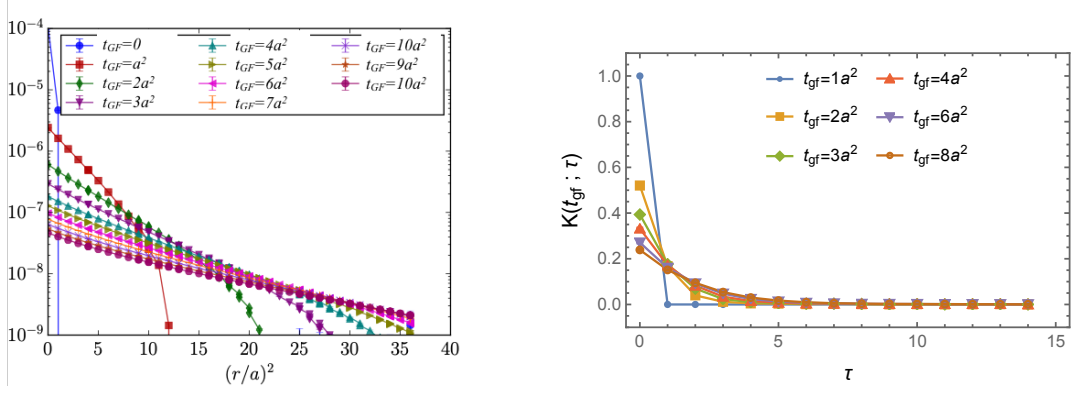


Figure 2: (Left) correlation of the topological charge density $\langle q(r)q(0) \rangle$ computed with t^{gf} and (right) diffusion kernel $K(t_2^{\text{gf}} - t_1^{\text{gf}}; \tau)$ (12).

We model this Euclidean-time diffusion effect of the gradient flow by

$$q(t_2^{\text{gf}}; \tau) = \int dt' K(t_2^{\text{gf}} - t_1^{\text{gf}}; |\tau - \tau'|) q(t_1^{\text{gf}}; \tau') \quad (11)$$

where $K(t_2^{\text{gf}} - t_1^{\text{gf}}; |\tau - \tau'|)$ is the diffusion kernel that can be extracted from Fourier-transformed correlations of the topological charge

$$K(t_2^{\text{gf}} - t_1^{\text{gf}}; \tau) = \frac{1}{L_t} \sum_k e^{i\omega_k \tau} \sqrt{\frac{\tilde{\chi}(t_2^{\text{gf}}; \omega_k)}{\tilde{\chi}(t_1^{\text{gf}}; \omega_k)}}, \quad \tilde{\chi}(t^{\text{gf}}; \omega_k) = \sum_{\tau} e^{-i\omega_k \tau} \langle q(t^{\text{gf}}; \tau) q(t^{\text{gf}}; 0) \rangle, \quad (12)$$

where the frequency $\omega_k = \frac{2\pi}{L_t} k$. Numerical results for kernel $K(t_2^{\text{gf}} - t_1^{\text{gf}}; |\tau|)$ are shown in Fig. 2, illustrating how the diffusion profile widens with increasing gradient flow time t^{gf} . Similarly, the effect of “diffusion” on the three-point correlation function (8) can be written as

$$\tilde{C}_3(t^{\text{gf}}; t_f, \tau) = \sum_{\tau'} K(t^{\text{gf}}; |\tau - \tau'|) C_3(t_f, \tau'), \quad (13)$$

where $C_3(t_f, \tau)$ is the correlation function that would be computed with a strictly local definition of the topological charge $q(\tau)$. Unfortunately, this diffusion mixes the neutron EDM signal with contributions from unwanted regions $\tau \leq 0$ and $\tau \geq t_f$, which we model as

$$C_{3pt}(\tau, t_f) = \begin{cases} a_0 e^{-E_0 t_f} (d_n + c_1 e^{-\Delta E_1 \tau} + c_1 e^{-\Delta E_1 (t_f - \tau)} + c_2 e^{-\Delta E_1 t_f}), & 0 < \tau < t_f, \\ C_{ext} e^{-E_0 t_f} e^{E_{ext} \tau}, & \tau \leq 0, \\ C_{ext} e^{-E_0 t_f} e^{-E_{ext}(\tau - t_f)}, & t_f \leq \tau. \end{cases} \quad (14)$$

The first line corresponds to the matrix element where the gluon operator is located between the source and sink. The second and the third lines represent the contributions from contact terms ($\tau = 0$ or $\tau = t_f$) and ‘‘crossed’’ regions with $q(\tau)$ located outside of the source-sink time interval.

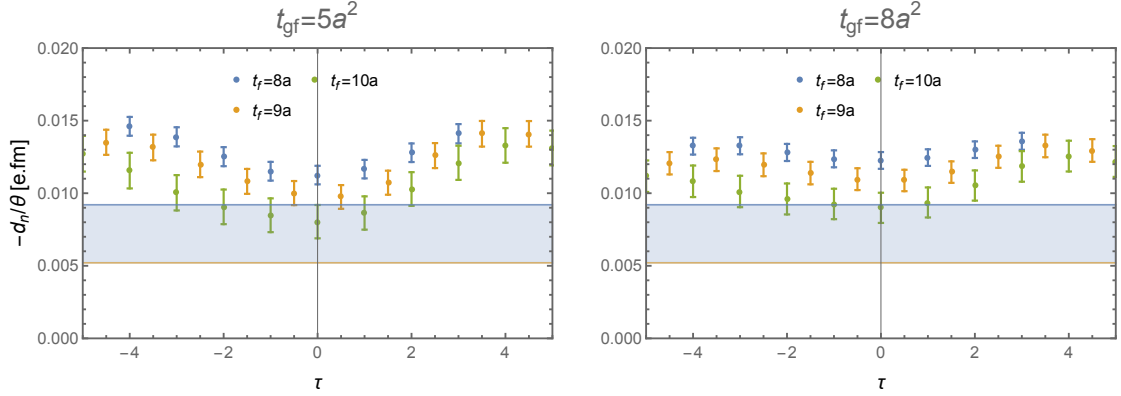


Figure 3: Fits of combined Euclidean-time (14) and gradient flow-time dependence (13) of lattice nEDM correlation functions. The band is the fit result using Eq. (14).

We perform a fit of three-point (8) data to ansatz (14) joint with a two-state fit of two-point neutron data to constrain ground- and excited-state energies $E_0, E_0 + \Delta E_1$. For the former, we select data with with longer range $8a \leq t_f \leq 10a$ and $5a^2 \leq t^{gf} \leq 8a^2$. The fit result for the ground-state EDM d_n/θ is shown in Fig. (3). We obtain the following values at the two pion masses

$$\begin{aligned} [d_n/\theta]_{340\text{MeV}} &= -0.0072(20)^{\text{stat}}, \\ [d_n/\theta]_{432\text{MeV}} &= -0.0060(20)^{\text{stat}}. \end{aligned}$$

Using chiral prediction $d_n(m_\pi^2) \sim c_1 m_\pi^2 + c_2 m_\pi^2 \log(m_\pi^2)$, we can obtain only a tentative estimate of the value at the physical point $(d_n/\theta)_{\text{lin.}+\log.}^{\text{phys}} = -0.0036(21)^{\text{stat}}$. The uncertainty of the extrapolation is substantially constrained by chiral symmetry in our EDM calculation.

4. Summary

In this work, we have calculated the neutron EDM employing the background field method on two gauge ensembles with chirally symmetric quarks and pion masses ≈ 340 and 420 MeV. Unlike in the traditional form-factor approach, we calculate the forward matrix element of the topological charge density in a simultaneously spin- and electrically-polarized nucleon state. This method is instrumental to limit the growth of the stochastic noise from the global topological charge as the

physical volume of a lattice increases. Without the need to extrapolate in the momentum transfer $Q^2 \rightarrow 0$, the systematic uncertainty can be further dramatically reduced.

The main obstacle in using this method is the difficulty of determining topological charge density. In this work, we have used the field-theoretical definition from the gluon fields combined with gradient flow. However, gradient flow leads to “diffusion” in Euclidean time and mixing of the nEDM signal with contact terms and contributions from $n\bar{n}$ -pair states. We have implemented the numerical procedure to extract the diffusion kernel from lattice data and incorporate it in the fits of correlators of the nucleon and the topological charge density. With only two pion mass points available, we could perform only a tentative estimate of the physical-point value. Another point at lighter pion mass $m_\pi \approx 250$ MeV is currently being investigated.

We plan to explore the fermionic definition [11, 25], which may be especially advantageous when combined with the low-mode approximation for neutron correlation function. Further, this method can be easily applied to other \mathcal{CP} operators, and might be especially beneficial for the nEDM induced by Weinberg’s three-gluon operator and 4-quark \mathcal{CP} operators.

Acknowledgments

The research reported in this work made use of computing and long-term storage facilities provided by the USQCD Collaboration, which are funded by the Office of Science of the U.S. Department of Energy, and the Hokusai supercomputer of the RIKEN ACCC facility. We are grateful for the gauge configurations provided by the RBC/UKQCD collaboration. SS and FH are supported by the National Science Foundation under CAREER Award PHY-1847893. Any opinions, findings, and conclusions or recommendations expressed in this material are those of the author(s) and do not necessarily reflect the views of the National Science Foundation. HO is supported in part by JSPS KAKENHI Grants No. 21K03554 and No. 22H00138. TB and MA were partially supported by the US DOE under the award DE-SC001033. TI is supported by U.S. Department of Energy (DOE) under award DE-SC0012704, SciDAC-5 LAB 22-2580, and also Laboratory Directed Research and Development (LDRD No. 23-051) of BNL and RIKEN BNL Research Center.

References

- [1] C. A. Baker et al., Phys. Rev. Lett. **97**, 131801 (2006), hep-ex/0602020.
- [2] B. Graner, Y. Chen, E. G. Lindahl, and B. R. Heckel, Phys. Rev. Lett. **116**, 161601 (2016), 1601.04339, [Erratum: Phys.Rev.Lett. 119, 119901 (2017)].
- [3] E. Shintani et al., Phys.Rev. **D72**, 014504 (2005), hep-lat/0505022.
- [4] F. Berruto, T. Blum, K. Orginos, and A. Soni, Phys.Rev. **D73**, 054509 (2006), hep-lat/0512004.
- [5] R. Horsley et al., (2008), 0808.1428.
- [6] F. K. Guo et al., Phys. Rev. Lett. **115**, 062001 (2015), 1502.02295.
- [7] C. Alexandrou et al., Phys. Rev. D **93**, 074503 (2016), 1510.05823.

- [8] E. Shintani, T. Blum, T. Izubuchi, and A. Soni, Phys. Rev. **D93**, 094503 (2016), 1512.00566.
- [9] M. Abramczyk et al., Phys. Rev. D **96**, 014501 (2017), 1701.07792.
- [10] J. Dragos, T. Luu, A. Shindler, J. de Vries, and A. Yousif, Phys. Rev. C **103**, 015202 (2021), 1902.03254.
- [11] C. Alexandrou, A. Athenodorou, K. Hadjiyiannakou, and A. Todaro, Phys. Rev. D **103**, 054501 (2021), 2011.01084.
- [12] T. Bhattacharya, V. Cirigliano, R. Gupta, E. Mereghetti, and B. Yoon, Phys. Rev. D **103**, 114507 (2021), 2101.07230.
- [13] J. Liang et al., (2023), 2301.04331.
- [14] E. Shintani et al., Phys. Rev. D **75**, 034507 (2007), hep-lat/0611032.
- [15] E. Shintani, S. Aoki, and Y. Kuramashi, Phys. Rev. D **78**, 014503 (2008), 0803.0797.
- [16] T. Izubuchi, H. Ohki, and S. Syritsyn, PoS **LATTICE2019**, 290 (2020), 2004.10449.
- [17] T. Izubuchi et al., PoS **LATTICE2007**, 106 (2007), 0802.1470.
- [18] W. Detmold, B. C. Tiburzi, and A. Walker-Loud, Phys. Rev. D **79**, 094505 (2009), 0904.1586.
- [19] W. Detmold, B. C. Tiburzi, and A. Walker-Loud, Phys. Rev. D **81**, 054502 (2010), 1001.1131.
- [20] C. Bouchard, C. C. Chang, T. Kurth, K. Orginos, and A. Walker-Loud, Phys. Rev. D **96**, 014504 (2017), 1612.06963.
- [21] T. Blum et al., Phys. Rev. D **93**, 074505 (2016), 1411.7017.
- [22] E. Shintani et al., Phys. Rev. **D91**, 114511 (2015), 1402.0244.
- [23] P. de Forcrand, M. Garcia Perez, and I.-O. Stamatescu, Nucl. Phys. **B499**, 409 (1997), hep-lat/9701012.
- [24] M. Lüscher, JHEP **08**, 071 (2010), 1006.4518, [Erratum: JHEP 03, 092 (2014)].
- [25] M. Lüscher and P. Weisz, Eur. Phys. J. C **81**, 519 (2021), 2103.15440.